



Atrium Health

Clinical Uses and Potential Future Applications of SGRT

Ryan Foster, PhD

Chief Physicist

Atrium Health/LCI NorthEast

Disclosures

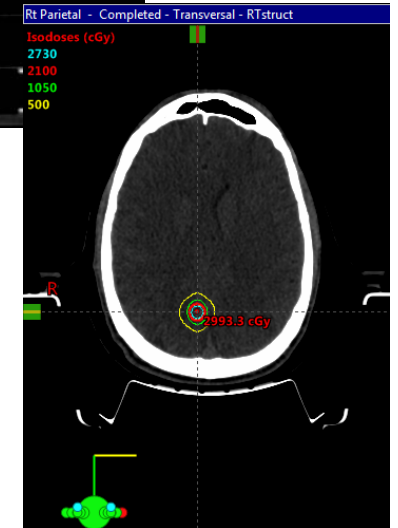
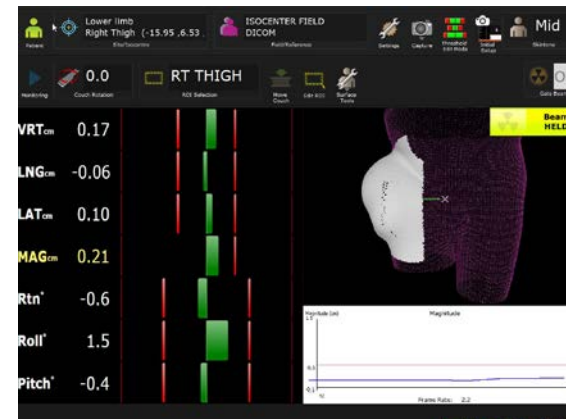
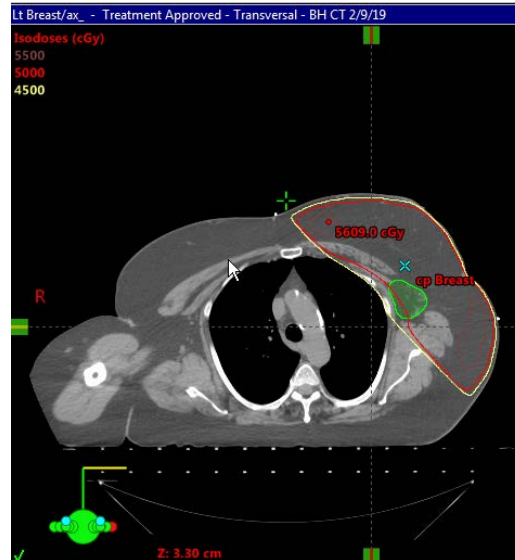
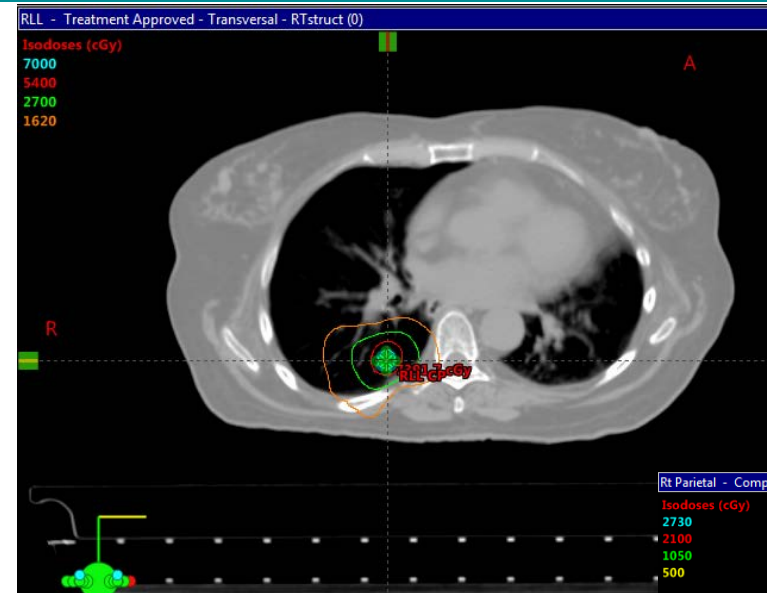
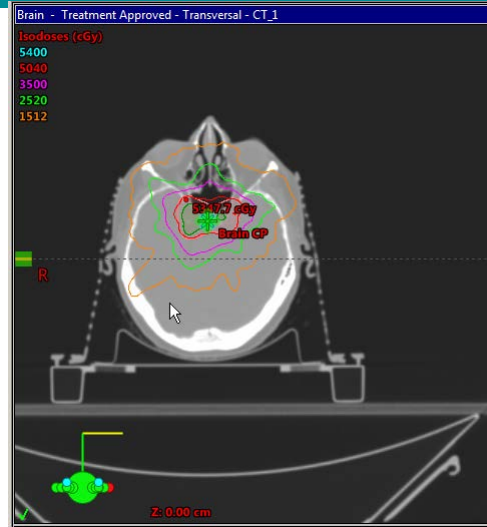
- Nothing to disclose

Objectives

- Understand the clinical uses of SGRT
- Understand the advantages and disadvantages of SGRT for various treatment sites
- Discuss potential future uses of SGRT

Disease sites with published/presented data

- Breast
- H&N
- SRS
- Thorax/abdomen
- Extremities
- Pelvis



Whole Breast Setup

Clinical evaluation of interfractional variations for whole breast radiotherapy using 3-dimensional surface imaging

Amish P. Shah PhD*, Tomas Dvorak MD, Michael S. Curry MS,
Daniel J. Buchholz MD, Sanford L. Meeks PhD

Department of Radiation Oncology, MD Anderson Cancer Center Orlando, Orlando, Florida

- Shah et al. PRO 2013
- Evaluated SGRT vs skin marks for setup
- Performed dosimetric evaluation

Table 1 Mean setup errors detected by the surface-based imaging system relative to alignment based on skin marks and lasers for all patients (n = 50)

	No. of treatment fractions	Vertical (mm)	Longitudinal (mm)	Lateral (mm)	3D vector (mm)
Average displacement (including nature of displacements)	1258	0.08	-0.20	-0.62	6.35
Average displacement (absolute value)	1258	4.09	2.67	2.59	6.35
Maximum individual average (absolute value)	1258	11.99	6.88	5.31	13.22
Minimum individual average (absolute value)	1258	0.91	0.82	0.80	2.76

Average values given as mean of individual means. Maximum and minimum values given as individual means of each patient. 3D, 3-dimensional.

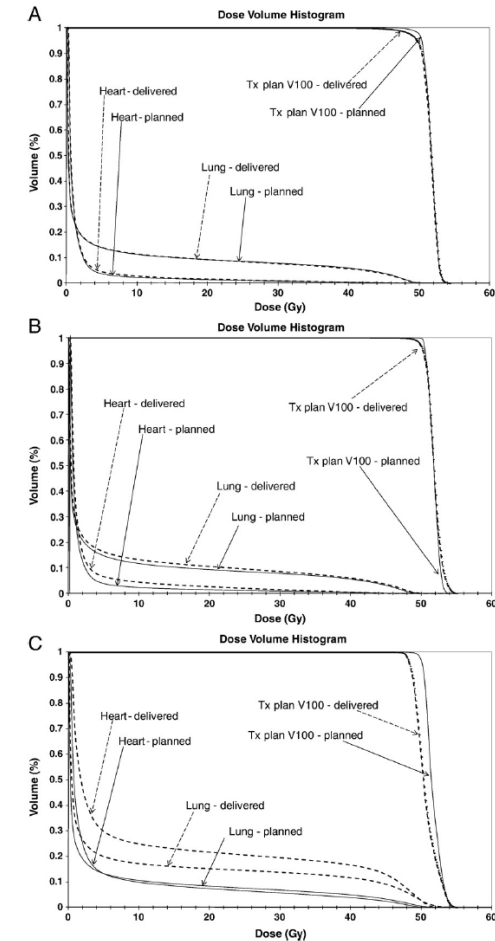


Figure 5 Planned and delivered dose-volume histograms of heart, lung, and volume of prescription isodose line from the treatment plan for (A) patient (No.7) with moderate AlignRT offsets from skin marks; (B) patient (No. 32) with excessive AlignRT offsets from skin marks (data displayed in Fig 3); and (C) left-sided breast cancer patient's treatment (Tx) plan, combined with a separate patient's daily offsets in order to display a possible "worst-case" scenario from daily laser and skin mark alignments with large systematic error.

CHRISTOPH BERT, M.S.,^{*†} KATHERINE G. METHEANY, B.S.,[†] KAREN P. DOPPKE, M.S.,[†]
ALPHONSE G. TAGHIAN, M.D., PH.D.,[†] SIMON N. POWELL, M.D., PH.D.,[†]
AND GEORGE T.Y. CHEN, PH.D.[†]

^{*}Abteilung Biophysik, Gesellschaft für Schwerionenforschung, Darmstadt, Germany; and [†]Department of Radiation Oncology, Massachusetts General Hospital and Harvard Medical School, Boston, MA

- Bert et al. IJROBP 2006
- Free breathing
- Evaluated SGRT for setup for accelerated partial breast irradiation (APBI)
- Compared to lasers and port films

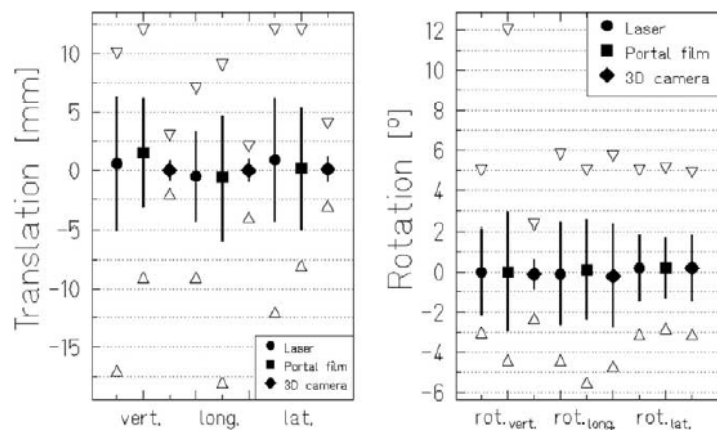


Fig. 7. Mean \pm standard deviation with minimum (Δ) and maximum (∇) of the couch shift required to bring the corresponding surface model back to reference. Data are from 9 patients, and 44 fractions were analyzed.

Table 1. Three-dimensional displacement (in mm) as recommended by the alignment procedure

Surface model	Mean	Standard deviation	Minimum	Maximum
Laser	7.3	4.4	1	17.6
Treatment	7.6	4.2	1.7	19.3
Virtual 3D alignment	1	1.2	0	4.2

DIBH – Clinical Results

- Zagar et al. IJROBP 2017
- Prospective trial evaluating utility of DIBH for preventing cardiac perfusion defects
- 20 patients evaluated

Utility of Deep Inspiration Breath Hold for Left-Sided Breast Radiation Therapy in Preventing Early Cardiac Perfusion Defects: A Prospective Study

Timothy M. Zagar, MD,^{*} Orit Kaidar-Person, MD,^{*} Xiaoli Tang, PhD,[†] Ellen E. Jones, MD,^{*} Jason Matney, MS,^{*} Shiva K. Das, PhD,^{*} Rebecca L. Green, MS,^{*} Arif Sheikh, MD,[‡] Amir H. Khandani, MD,[§] William H. McCartney, MD,[§] Jorge Daniel Oldan, MD,[§] Terence Z. Wong, MD, PhD,[§] and Lawrence B. Marks, MD^{*}

Departments of ^{*}Radiation Oncology, and [§]Radiology, University of North Carolina, Chapel Hill, North Carolina; [†]Memorial Sloan Kettering Cancer Center, West Harrison; and [‡]Department of Radiology, Columbia University; New York, New York

Table 2 Radiation doses and target volumes

Characteristics	No. of patients
Total prescribed dose (cGy) [*] (fraction number)	
4272 (16)	10
4600 (23)	6
5000 (25)	4
Prescribed boost dose (cGy) [†] (fraction number)	
1000 (5)	11
1200 (6)	2
1600 (8)	6
Internal mammary chain RT (superiorly placed nodes)	7
Supraclavicular RT field	5
Whole axillary RT field	0

^{*} To whole breast/chest wall

[†] Tumor bed/scar. In 18 patients an electron boost was used; in 1 patient photon boost was used.

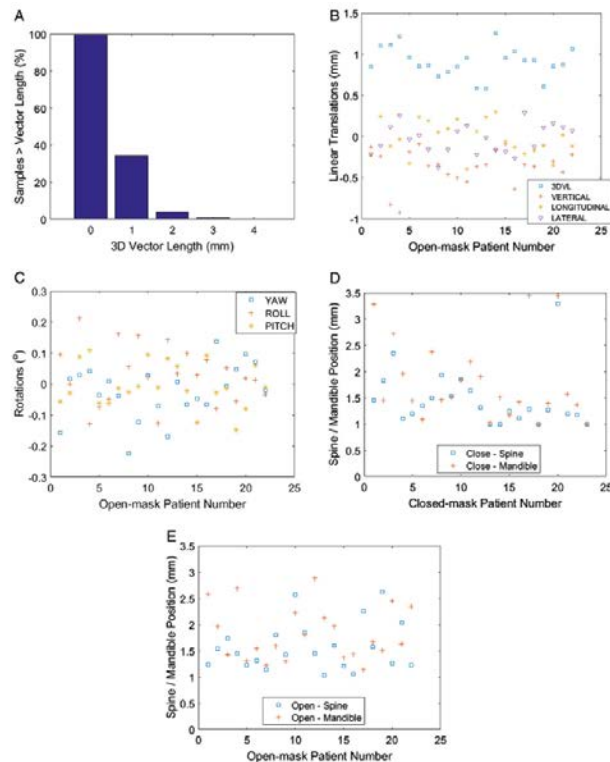
Table 3 Dosimetric parameters of radiation therapy (RT) plans

Parameters	No. (range)
Median % D95 tumor bed [*]	100.8 (92.3-102.4)
Median mean heart dose (cGy)	94 (56-200)
Median heart V25 _{Gy}	0 (0-0.1)
Median ipsilateral lung V20 _{Gy}	15 (4-31)

^{*} Minimum dose to the “hottest” 95% of the tumor bed, in patients with intact breast.

By the use of early imaging changes after RT as a surrogate marker for RT-associated heart injury, the present study suggests that DIBH with conformal cardiac blocking is an effective means to mitigate cardiac injury. At 6 months post RT, none of the patients in this study had a new RT-associated perfusion or wall motion defects on cardiac SPECT. This rate of cardiac perfusion abnormalities after RT is lower than the 27% rate reported by Marks et al (9) (used as our historical control during protocol design) and is also lower than the rates reported by others (8, 11, 12).

- Wiant et al. PRO 2016
- Prospective evaluation of open face masks for H&N RT
- Monitored intra-fraction motion for open-face masks using SGRT

**Table 2** Intrafraction motion group mean values

	3DVL	Vertical	Longitudinal	Lateral	Yaw	Roll	Pitch
Mean (mm)	0.9	-0.4	0.0	0.0	0.0	0.0	0.0
1 SD (mm)	0.5	0.5	0.7	0.5	0.3	0.3	0.2
Range (mm)	0.1 to 3.5	-3.0 to 1.7	-2.7 to 3.5	-2.2 to 3.0	-1.3 to 1.3	-1.8 to 1.4	-0.9 to 1.1
Range of means (mm)	0.6 to 1.3	-0.9 to -0.1	-0.4 to 0.3	-0.4 to 0.3	-0.2 to 0.1	-0.1 to 0.2	-0.1 to 0.1

3DVL, 3-dimensional vector length; SD, standard deviation.

Figure 2 (A) Percent of 568 total monitored fractions with 3-dimensional vector length (3DVL) greater than the listed value for the open-mask group. Mean values for the open-mask group over all fractions for (B) 3DVL and (C) rotations. Mean spinal canal and mandible contour expansions that covered the structures in the (D) closed-mask group and (E) open-mask group.

Why use SGRT for SRS and SBRT?

- Treatments with small margins and sharp dose gradients
- Allow smaller margins?
- Benign conditions or pediatric patients – reduce imaging dose
- Pediatrics or non-compliant patients – reduce margins and eliminate need for anesthesia
- Facilitate breath hold lung/abdomen SBRT

SRS

- Li et al. Med Phys 2011
- SGRT used to verify setup at treatment angles and for motion monitoring
- CBCT used as standard for IGRT
- Compared frame-based SRS with frameless



FIG. 2. The noninvasive head immobilization (PinPoint[®]) system used in this frameless SRT/SRS procedure. (1) A carbon-fiber couch board with a head support, (2) a patient-specific head mold, (3) a patient-specific mouthpiece, (4) an adjustable, rigid connector, and (5) a metal arch, which is locked to a couch board (1).

Motion monitoring for cranial frameless stereotactic radiosurgery using video-based three-dimensional optical surface imaging

Guang Li,^{a)} Åse Ballangrud, Li Cheng Kuo, Hyejoo Kang, Assen Kirov, and Michael Lovelock
Department of Medical Physics, Memorial Sloan-Kettering Cancer Center, 1275 York Avenue, New York, New York 10065

Yoshiya Yamada
Department of Radiation Oncology, Memorial Sloan-Kettering Cancer Center, 1275 York Avenue, New York, New York 10065

James Mechalakos and Howard Amols
Department of Medical Physics, Memorial Sloan-Kettering Cancer Center, 1275 York Avenue, New York, New York 10065

TABLE I. Average head motion for frame-based SRS patients at all treatment couch angles using AlignRT surface imaging. Motion magnitude is defined as $\sqrt{x_m^2 + y_m^2 + z_m^2}$ (m = translation or rotation).

Treatment	Patient	Number of lesions	Age	Sex	Translational magnitude (mm)	SD ^a	Rotational magnitude (°)	SD ^a
Frame-based SRS	1	3	59	F	0.36	0.23	0.28	0.23
	2	2	48	F	0.29	0.16	0.19	0.14
	3	2	65	M	0.29	0.19	0.20	0.18
	4	1	53	F	0.20	0.14	0.23	0.15
	5	2	56	F	0.25	0.15	0.14	0.11
	6	2	67	F	0.33	0.20	0.16	0.13
	7	1	70	M	0.19	0.12	0.18	0.11
	8	1	45	M	0.29	0.15	0.16	0.10
	9	3	74	M	0.32	0.21	0.43	0.37
	10	1	33	F	0.19	0.14	0.18	0.16
	11	1	64	F	0.13	0.07	0.08	0.05
	Average	1.7	58		0.3	0.2	0.2	0.2
	SD ^a	0.8	12		0.1	0.1	0.1	0.1
	RMS ^c	1.9	59		0.3	0.2	0.3	0.2

TABLE II. Setup verification and head motion of frameless SRT/SRS patients averaged at all treatment couch angles using AlignRT surface imaging. Motion magnitude is defined as $\sqrt{x_m^2 + y_m^2 + z_m^2}$ (m = translation or rotation).

Treatment	Patient	Fraction number	Age	Sex	Setup verification		Near-real-time motion monitoring			
					Translation difference ^a (mm)	SD ^b	Translation magnitude (mm)	SD ^b	Rotation magnitude (°)	SD ^b
Frameless SRT	1	1	68	F	0.9	0.3	0.25	0.16	0.20	0.12
		2			0.8	0.3	0.19	0.08	0.10	0.05
		3			1.1	0.7	0.35	0.24	0.17	0.15
	2	1	48	F	0.7	0.2	0.32	0.21	0.10	0.05
		2			0.8	0.6	0.15	0.08	0.12	0.06
		3			0.4	0.2	0.37	0.17	0.19	0.09
		4			1.1	0.2	0.52	0.30	0.19	0.12
		5			1.1	0.2	0.28	0.12	0.18	0.10
Frameless SRS	1	1	71	M	0.9	0.1	0.51	0.26	0.37	0.23
	2	1	38	F	0.8	0.3	0.37	0.20	0.29	0.14
	Mean				0.9	0.3	0.3	0.2	0.2	0.1
	SD ^b				0.2	0.2	0.1	0.1	0.1	0.1
	RMS ^c				0.9	0.4	0.4	0.2	0.2	0.1

^aSetup verification: the values (in mm) are absolute vector distances calculated using Eq. (2) and averaged at all couch angles.

^bSD, standard deviation.

^cRMS, root mean square.

Laura I. Cerviño PhD*, Nicole Detorie PhD, Matthew Taylor BS, Joshua D. Lawson MD, Taylor Harry BS, Kevin T. Murphy MD, Arno J. Mundt MD, Steve B. Jiang PhD, Todd A. Pawlicki PhD

Department of Radiation Oncology, University of California San Diego, La Jolla, California

- Cerviño et al. PRO 2012
- Frameless and maskless SRS monitored with SGRT – 23 patients
- Evaluated CBCT – SGRT agreement for setup
- Interrupted treatment if intra-fraction motion exceeded 1 – 2 mm (margin dependent)

Shifts calculated based on CBCT after the initial setup with AlignRT were -0.8 mm, 1.8 mm, and 0.0 mm in the lateral, anterior-posterior (AP), and superior-inferior (SI) directions, respectively. For our first patient, the shifts

Eight patients needed repositioning during the treatment.

In most of these cases, repositioning was required when a treatment field included a couch rotation. In 3 cases, patients fell asleep and also needed repositioning during treatment.

beam hold was initiated at least once for 15 patients. In most cases, the patient movement would naturally return back under the movement threshold value. The worst cases were the 2 patients who fell asleep, where the treatment was interrupted 10 and 14 times. Although the average number



Figure 1 An example of a patient-specific head mold made out of expandable foam that conforms to the patient's head (CDR Systems, Inc, Calgary, Alberta, Canada).

SRS Clinical Outcomes

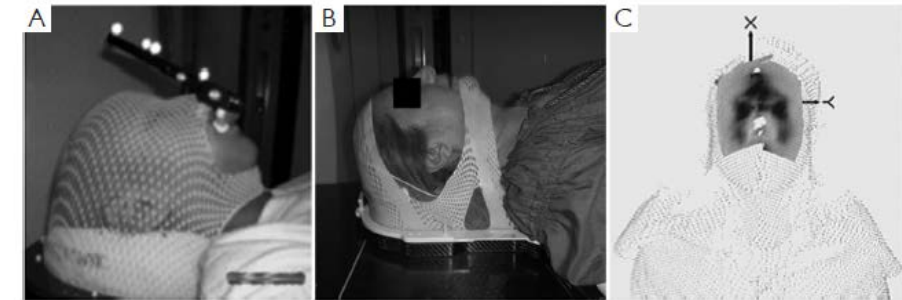
Frameless, real-time, surface imaging-guided radiosurgery: update on clinical outcomes for brain metastases

Nhat-Long L. Pham, Pranav V. Reddy, James D. Murphy, Parag Sanghvi, Jona A. Hattangadi-Gluth, Grace Gwe-Ya Kim, Laura Cervino, Todd Pawlicki, Kevin T. Murphy

Department of Radiation Medicine and Applied Science, University of California, San Diego, La Jolla, CA 92093, USA

Correspondence to: Kevin T. Murphy, MD. Department of Radiation Medicine and Applied Science, University of California, San Diego, La Jolla, California, 3960 Health Sciences Dr., MC0865, La Jolla, CA 92093, USA. Email: kevinmurphy@ucsd.edu.

- Pham et al. Trans Canc Res 2014
- Reported clinical outcomes for frameless SGRT guided SRS
- 163 patients with 490 lesions and 45 post-op cavities



findings that SIG-RS for treating brain metastases can produce clinical outcomes comparable to those for conventional frame-based and frameless SRS techniques. At the same time, SIG-RS setup provides better comfort with an open-faced mask, and allows continuous non-ionizing tracking during the treatment delivery time.

Table 2 Comparison of local control and survival rates in retrospective studies of brain metastases treated with radiosurgery reporting kaplan-meier data^a

Study	Treatment system	Patients, n	Crude LC, %	Actuarial 1-yr LC, %	Actuarial 1-yr OS, %
Schomas <i>et al.</i> (19) [2005]	Frame-based LINAC	80	91	89	33
Bhatnagar <i>et al.</i> (18) [2006]	Frame-based Gamma Knife	205	***	71	37 ^b
Breneman <i>et al.</i> (6) [2009]	Frameless LINAC	53	***	80	44
Nath <i>et al.</i> (7) [2010]	Frameless LINAC	65	88	76	40
Pan <i>et al.</i> (17) [2012]	Frameless, surface-imaging guided LINAC	44	85	76	38
Present series	Frameless, surface-imaging guided LINAC	163	85	79	56

^a, LC indicates local control; LINAC, linear accelerator; ***, not reported; ^b, estimated from Kaplan-Meier curve.

Thorax/Abdomen

- External – Internal Correlation?
- Glide-Hurst et al. Med Phys 2011
- Coupled SGRT with on-board fluoro

TABLE I. Tracking performance of the motion platform as measured by on-board kV fluoroscopy and surface imaging.

Expected	Period (s)		Amplitude (cm)		Latency (s)
	Surface imaging Mean \pm Stdev	Fluoroscopy Mean \pm Stdev	Surface imaging Mean \pm Stdev		
3.33	3.33 \pm 0.07	3.31 \pm 0.08	1.00 \pm 0.01		0.62
4.00	4.00 \pm 0.04	3.97 \pm 0.10	1.01 \pm 0.00		0.66
5.00	4.99 \pm 0.07	4.98 \pm 0.15	1.00 \pm 0.00		0.63
					0.64 \pm 0.02

TABLE II. The internal (measured via fluoroscopy) to external (measured via surface imaging cameras) correlation (the Pearson correlation coefficient) before and after latency correction for three patient breathing traces simulated with the motion platform. All latency-corrected correlations were statistically significant ($p < 0.001$).

Breathing trace	Scaled tumor excursion (Mean \pm Stdev, cm)	Uncorrected Pearson r	Latency-corrected	
			Pearson r	RMSE (mm)
Trace 1	0.69 \pm 0.65	0.47	0.97	0.48
Trace 2	0.24 \pm 0.73	0.44	0.97	0.82
Trace 3	0.58 \pm 0.67	0.13	0.97	0.42

TABLE III. Patient-specific correlations between abdominal surface motion and superior–inferior internal motion (tumor and diaphragm) are presented. The internal structures were measured using fluoroscopy whereas external abdominal motion was measured via surface imaging cameras.

Patient	Treatment timepoint	Abdomen–diaphragm		Abdomen–tumor		Diaphragm–tumor	
		Pearson r	RMSE (mm)	Pearson r	RMSE (mm)	Pearson r	RMSE (mm)
1	Pre	0.94	1.19	0.90	1.91	0.95	1.35
	Post	0.92	1.04	0.96	1.02	0.95	1.13
2	Pre	0.99	0.73	0.96	1.01	0.95	1.15
	Post	0.98	0.93	0.93	1.34	0.93	1.35
3	Pre	0.96	2.99	0.83	3.37	0.87	2.95
	Post	0.85	5.01	0.73	1.43	0.91	0.86

Coupling surface cameras with on-board fluoroscopy: A feasibility study

Carri K. Glide-Hurst
Department of Radiation Oncology, Henry Ford Health Systems, Detroit, Michigan 48202

Dan Ionascu
Department of Radiation Oncology, William Beaumont Hospital, Royal Oak, Michigan 48073

Ross Berbeco
Department of Radiation Oncology, Dana-Farber/Brigham and Women's Cancer Center and Harvard Medical School, Boston, Massachusetts 02115

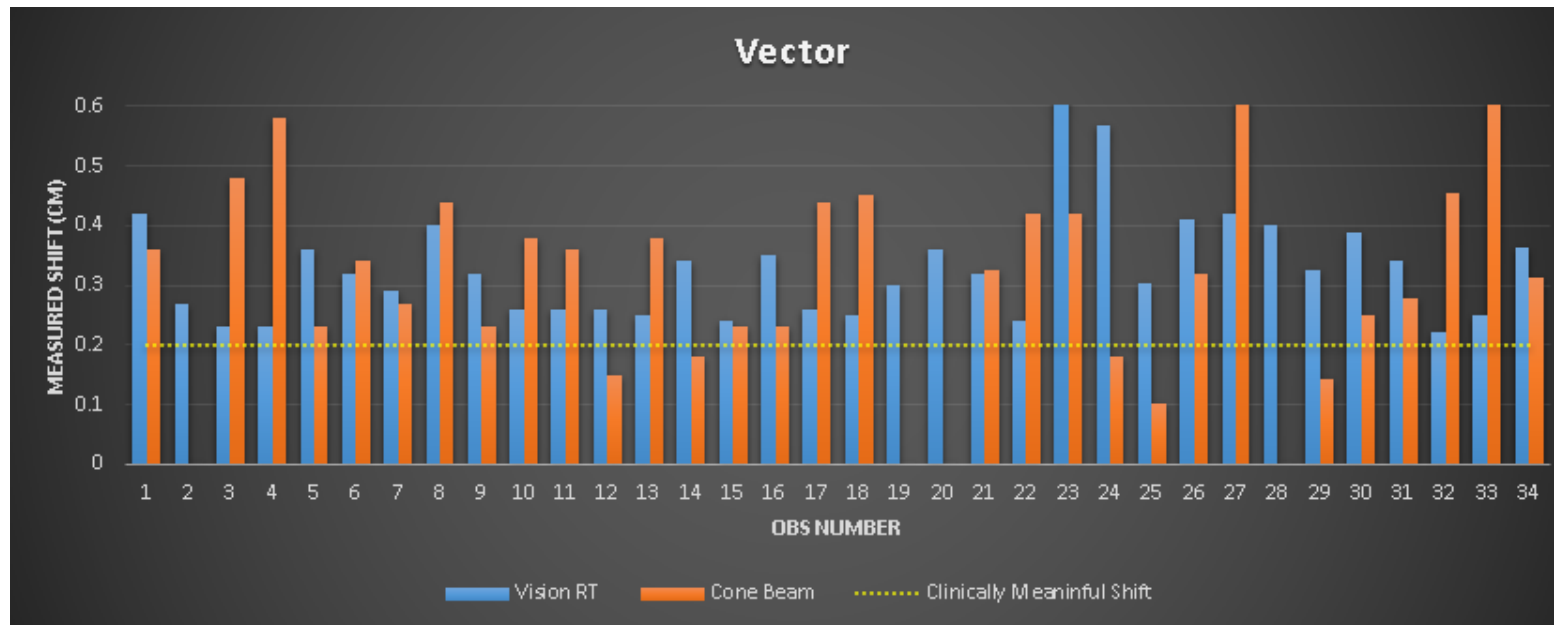
Di Yan
Department of Radiation Oncology, William Beaumont Hospital, Royal Oak, Michigan 48073

Thorax/Abdomen

- Heinzerling et al. ASTRO 2017 abstract
- Manuscript under review
- Intra-fraction monitoring of SBRT patients
- 2 mm/2° tolerance – Intra-fraction CBCT
- No significant difference seen in mean 3D vector shifts from SGRT and CBCT

Use of 3D Optical Surface Mapping for Quantification of Interfraction Set up Error and Intrafraction Motion during Stereotactic Body Radiation Therapy Treatments of the Lung and Abdomen

J.H. Heinzerling,^{1,2} C.J. Hampton,² M. Robinson,³ M. Bright,² J.T. Symanowski,³ B.J. Moeller,^{1,2} K. Mileham,² S.H. Burri,^{2,4} and R.D. Foster²; ¹*Southeast Radiation Oncology Group, Levine Cancer Institute, Carolinas HealthCare System, Charlotte, NC*, ²*Levine Cancer Institute: Carolinas HealthCare System, Charlotte, NC*, ³*Department of Biostatistics, Levine Cancer Institute, Carolinas Healthcare System, Charlotte, NC*, ⁴*Southeast Radiation Oncology Group, Levine Cancer Institute, Charlotte, NC*



Summary of other treatment sites with published data

- Pelvis – Krengli et al. Radiation Oncology 2016
- Extremities – Gierga et al. PRO 2014
- Setup accuracy – Walter et al. Radiation Oncology 2016, Stanley et al. JACMP 2017

Future Directions

- SGRT only for initial patient set up – eliminate tattoos (some places have done this already)
- Patient identification applications
- Maskless H&N and SRS (claustrophobic patients)
- Use intra-fraction motion data to determine margins

Disadvantages of SGRT

- Require patient surface to be visible – could limit types of immobilization used
- Gantry, imaging arms etc can block the camera's view of the patient
- Surfaces without much variation can be challenging to track
- Surface is not always a reliable surrogate for internal tumor position
- Potential mismatches in surfaces generated from a CT dataset and that reconstructed by SGRT

Conclusions

- SGRT is an attractive option for patient set-up and intra-fraction monitoring
- Can be used for almost any treatment site
- Uses visible light – no additional dose to the patient
- Sub-millimeter accuracy is achievable
- Surface – internal correlation is still under investigation

